Zinc transporter 1 (ZNT1) expression on the cell surface is elaborately controlled by cellular zinc levels

AUTHOR(S):

Nishito, Yukina; Kambe, Taiho

JBC ARTICLE

Zinc transporter 1 (ZNT1) expression on the cell surface is elaborately controlled by cellular zinc levels

Received for publication, July 19, 2019, and in revised form, August 20, 2019 Published, Papers in Press, August 30, 2019, DOI 10.1074/jbc.RA119.010227

Yukina Nishito[1] and **Taiho Kambe**[2]

From the Division of Integrated Life Science, Graduate School of Biostudies, Kyoto University, Kyoto 606-8502, Japan

Edited by Mike Shipston

Zinc transporter 1 (ZNT1) is the only zinc transporter predominantly located on the plasma membrane, where it plays a pivotal role exporting cytosolic zinc to the extracellular space. Numerous studies have focused on the physiological and pathological functions of ZNT1. However, its biochemical features remain poorly understood. Here, we investigated the regulation of ZNT1 expression in human and vertebrate cells, and found that ZNT1 expression is posttranslationally regulated by cellular zinc status. We observed that under zinc-sufficient conditions, ZNT1 accumulates on the plasma membrane, consistent with its zinc efflux function. In contrast, under zinc-deficient conditions, ZNT1 molecules on the plasma membrane were endocytosed and degraded through both the proteasomal and lysosomal pathways. Zinc-responsive ZNT1 expression corresponded with that of metallothionein, supporting the idea that ZNT1 and metallothionein cooperatively regulate cellular zinc homeostasis. ZNT1 is *N*-glycosylated on Asn^{299} in the extracellular loop between transmembrane domains V and VI, and this appears to be involved in the regulation of ZNT1 stability, as nonglycosylated ZNT1 is more stable. However, this posttranslational modification had no effect on ZNT1's ability to confer cellular resistance against high zinc levels or its subcellular localization. Our results provide molecular insights into ZNT1-mediated regulation of cellular zinc homeostasis, and indicate that the control of cellular and systemic zinc homeostasis via dynamic regulation of ZNT1 expression is more sophisticated than previously thought.

In vertebrates, cellular and systemic zinc homeostasis are maintained through its mobilization across the membranes by two zinc transporter family proteins, ZIP[3] and ZNT (1–3), which are located on the membranes of both the cell surface and intracellular compartments. Most ZIP proteins are on the plasma membrane and mobilize zinc from the extracellular space to the cytosol as zinc importers, and therefore, cells have a number of zinc entry routes (1–3). In contrast, most ZNT proteins are in intracellular compartments, and ZNT1 is the only ZNT protein that predominantly functions on the plasma membrane as a zinc efflux transporter (4–6), although other ZNT proteins can localize to the cell surface (7–9). Therefore, ZNT1 is a crucial regulator of cellular zinc homeostasis.

Discovered in 1995, ZNT1 was the first mammalian zinc transporter protein identified (4), and it is now known to play important roles in physiological and pathophysiological processes (10). ZNT1 protects cells from zinc toxicity by exporting cytosolic zinc into the extracellular space (11–13), which may be important for protecting neurons after transient forebrain ischemia (14, 15). Its functions in controlling cytosolic zinc levels regulate the activation of RAF-1, which is a signal transducer in the RAS-ERK pathway (16), which may protect cells from ischemia reperfusion (17). The functions of ZNT1 that control signaling are conserved among ZNT1 orthologs, because a *Caenorhabditis elegans* ortholog controls RAS-ERK signaling (18). ZNT1 is essential for embryonic development because it transports maternal zinc into the embryonic environment, and homozygous *znt1* knockout mice exhibit early embryonic death (19). In enterocytes, ZNT1 is located on the basolateral membrane, so probably facilitates zinc absorption by exporting it into portal blood (6, 10, 20). In addition to its functions as a zinc exporter, ZNT1 also plays regulatory roles, most of which are related to protein-protein interactions with ZNT1 in intracellular compartments. In the endoplasmic reticulum (ER), ZNT1 interacts with the β-subunit of the L-type calcium channel, which leads to a reduction in the cell surface expression of its pore-forming α_1-subunit (21). Moreover, its interaction with EVER proteins may be involved in the pathogenesis of *Epidermodysplasia verruciformis*, which is a rare autosomal recessive skin disease (OMIM 226400) (22). Taken together, these observations clearly highlight ZNT1's importance in cellular and systemic homeostatic control. However, the molecular feature of ZNT1 is relatively unknown.

This work was supported by a Grant-in-Aid for Scientific Research on Innovative Areas "Bio-metal" KAKENHI Grant 19H05768 (to T. K.) from the Ministry of Education, Culture, Sports, Science, and Technology, Japan, Grant-in-Aid for Scientific Research (B) KAKENHI Grants 15H04501 and 19H02883 (to T. K.) from the Japan Society for the Promotion of Science (to T. K.), a Grant-in-Aid for JSPS Research Fellow KAKENHI Grant 17J09455 (to Y. N.), and grants from the Fuji Foundation for Protein Research, Ito Foundation, Sugiyama Chemical & Industrial Laboratory, Kao Melanin Workshop, and the Cosmetology Research Foundation (to T. K.). The authors declare that they have no conflicts of interest with the contents of this article.

This article contains Fig. S1 and Tables S1 and S2.

The amino acid sequence of this protein can be accessed through the DNA Databank of Japan under accession number BBM28213.1.

[1] Present address: Dept. of Analytical & Bioinorganic Chemistry, Kyoto Pharmaceutical University, Kyoto, Japan.

[2] To whom correspondence should be addressed. Tel.: 81-75-753-6273; Fax: 81-75-753-6274; E-mail: kambe1@kais.kyoto-u.ac.jp.

[3] The abbreviations used are: ZIP, Zrt/Irt-like protein; ZNT, zinc transporter; MT, metallothionein; MTF-1, metal-response element-binding transcription factor-1; FCS, fetal calf serum; CHX, cycloheximide; Dox, doxycycline; qPCR, quantitative PCR; ER, endoplasmic reticulum; MEF, mouse embryonic fibroblast; PNGase F, peptide *N*-glycosidase F; KO, knock-out; MDCK, Madin-Darby canine kidney cells; TPEN, *N*,*N*,*N*′,*N*′-Tetrakis(2-pyridylmethyl)ethylenediamine.

A well-known molecular feature of ZNT1 is that it is transcriptionally up-regulated in response to high zinc levels, and this is mediated through the binding of metal-response element-binding transcription factor-1 (MTF-1) to the metal-response elements in its promoter region (23–25). This transcriptional regulation in response to high zinc levels is similar to that of metallothionein (MT), which is also a target gene of MTF-1. However, other features of ZNT1 expression regulation still remain poorly understood. In this study, we investigated the molecular features and expression regulation of ZNT1 in human and vertebrate cells using an anti-ZNT1 mAb that we generated in previous studies (26).

Results

ZNT1 is N-glycosylated on the Asn^{299} residue, which neither affects the ability to confer resistance against high zinc levels nor the subcellular localization of ZNT1

We first confirmed whether our anti-ZNT1 mAb, which was generated against the C-terminal cytosolic portion of the protein, specifically detects ZNT1 using an N-terminally FLAG-tagged ZNT1 (FLAG-ZNT1) protein, because it detected ZNT1 at a greater molecular size than that calculated based on its cDNA in our previous study (26–28). The anti-ZNT1 mAb detected FLAG-ZNT1 stably expressed in DT40 cells deficient in *znt1*, *mt*, and *znt4* (*znt1*$^{-/-}$*mt*$^{-/-}$*znt4*$^{-/-}$) (27, 29) as two bands (mainly ~75 and ~63 kDa) in immunoblotting (Fig. 1*A*, *left*), which was also detected in the same manner by an anti-FLAG antibody (Fig. 1*A*, *right*), indicating that both bands were specific to ZNT1. We conducted two experiments to investigate whether the presence of two bands may have been caused by variations in glycosylation. First, we treated a cell lysate prepared from *znt1*$^{-/-}$*mt*$^{-/-}$*znt4*$^{-/-}$ cells overexpressing FLAG-ZNT1 with PNGase F, which hydrolyzes all types of *N*-linked oligosaccharide structures. The PNGase F treatment shifted the ~75 kDa band of ZNT1 to ~63 kDa, indicating that the higher band is the *N*-glycosylated form of ZNT1 (Fig. 1*B*, *lane 4*). The ~63 kDa band was still higher than 55.3 kDa, the expected molecular mass of ZNT1, which could be attributed to the properties of the cytosolic histidine-rich loop. Second, because ZNT1 has a consensus motif for *N*-glycosylation (Asn^{299}–Ser^{300}–Thr^{301}) in extracellular loop 3 (EL3) between transmembrane domains V and VI, we constructed a nonglycosylated ZNT1 mutant in which the 299th Asn residue (Asn^{299}) was substituted with an Ala residue (ZNT1$_{N299A}$). Immunoblotting of ZNT1$_{N299A}$ only showed the ~63 kDa band (Fig. 1*B*, *lane 5*), clearly indicating that ZNT1 is *N*-glycosylated at Asn^{299}.

Then, we investigated the effect of *N*-glycosylation at Asn^{299} on ZNT1 functions, specifically its subcellular localization and ability to tolerate high zinc concentrations. The cell surface localization of the ZNT1$_{N299A}$ mutant was confirmed by immunofluorescence staining (Fig. 1*C*, *upper panels*) and a cell surface biotinylation assay (Fig. 1*C*, *lower panels*), indicating that *N*-glycosylation at Asn^{299} is unimportant for the subcellular localization of ZNT1. Because our previous results demonstrated that *znt1*$^{-/-}$*mt*$^{-/-}$*znt4*$^{-/-}$ cells can be used to evaluate ZNT1 zinc transport ability (27, 29), we examined the ability of the ZNT1$_{N299A}$ mutant in these cells. The ZNT1$_{N299A}$ mutant conferred resistance to *znt1*$^{-/-}$*mt*$^{-/-}$*znt4*$^{-/-}$ cells against high zinc concentrations, comparable with that of wildtype (WT) ZNT1 (Fig. 1*D*). These results indicate that *N*-glycosylation is unimportant in terms of ZNT1's ability to traffic to the cell surface or to confer cellular resistance against high zinc levels.

Characterization of endogenous ZNT1 in cultured human cells

Previous studies have revealed that ZNT1 plays crucial roles in reducing zinc toxicity when overexpressed (11–13), but its molecular characterization remains to be elucidated. We characterized ZNT1 using cultured human cells, in which the *ZNT1* gene was disrupted by CRISPR/Cas9-mediated genome editing. The loss of ZNT1 in chronic myelogenous leukemia haploid HAP1 or pancreatic cancer PANC1 cells was confirmed by immunoblotting using our anti-ZNT1 mAb (Fig. 2, *A* and *B*). The results of the genome editing were confirmed by genomic DNA sequencing (Fig. S1). In *ZNT1*-deficient cells, MT protein expression was significantly increased compared with that in WT cells (Fig. 2, *A* and *B*), suggesting that the loss of ZNT1 increases the cytosolic zinc contents. Treating the total cellular lysates with PNGase F shifted the ~75 kDa band of endogenous ZNT1 to the ~63 kDa band (Fig. 2, *C* and *D*), similar to the above experiment, confirming that endogenous ZNT1 is also *N*-glycosylated. The re-expression of ZNT1 in *ZNT1*-deficient PANC1 cells decreased MT induction to the basal level found in WT PANC1 cells but did neither by the expression of ZNT1$_{H43N}$ and ZNT1$_{H43A}$ mutants (Fig. 2*E*), both of which had lost their zinc transport ability, as described previously (26, 27). Consistent with these results, ZNT1 re-expression conferred resistance against high zinc concentrations but both the mutants did not (Fig. 2*F*). These results confirm that ZNT1 plays critical roles in reducing zinc toxicity by effluxing excess zinc.

ZNT1 has been shown to be located on the basolateral membrane (6, 10, 20), which was confirmed in this study. The cell surface biotinylation assay and Z-stack analysis of the immunofluorescence microscopy results revealed that endogenous ZNT1 was located on the basolateral membrane in polarized Caco2 cells (Fig. 2, *G* and *H*) and was *N*-glycosylated, indicating that *N*-glycosylation is a general modification of the ZNT1 protein (Fig. 2*I*).

Zinc-induced ZNT1 accumulation on the cell surface

ZNT1 mRNA expression increases in response to high zinc levels (23–25, 30), which was confirmed in hepatoma HepG2 cells by zinc supplementation (50 μM $ZnSO_4$) (Fig. 3*A*). Consistent with the increase in its mRNA expression, the expression of the ZNT1 protein also increased (Fig. 3*B*), but the time course of these increases during $ZnSO_4$ treatment differed. The ZNT1 expression at the protein level increased gradually up to 12 h, whereas its expression at the mRNA level increased for up to 3 h and decreased in 6 h. Therefore, we examined the expression of the ZNT1 protein at the post-translational level in more detail.

ZNT1 protein expression was increased in HepG2 cells by low levels of zinc supplementation (20 μM $ZnSO_4$; Fig. 3*C*)

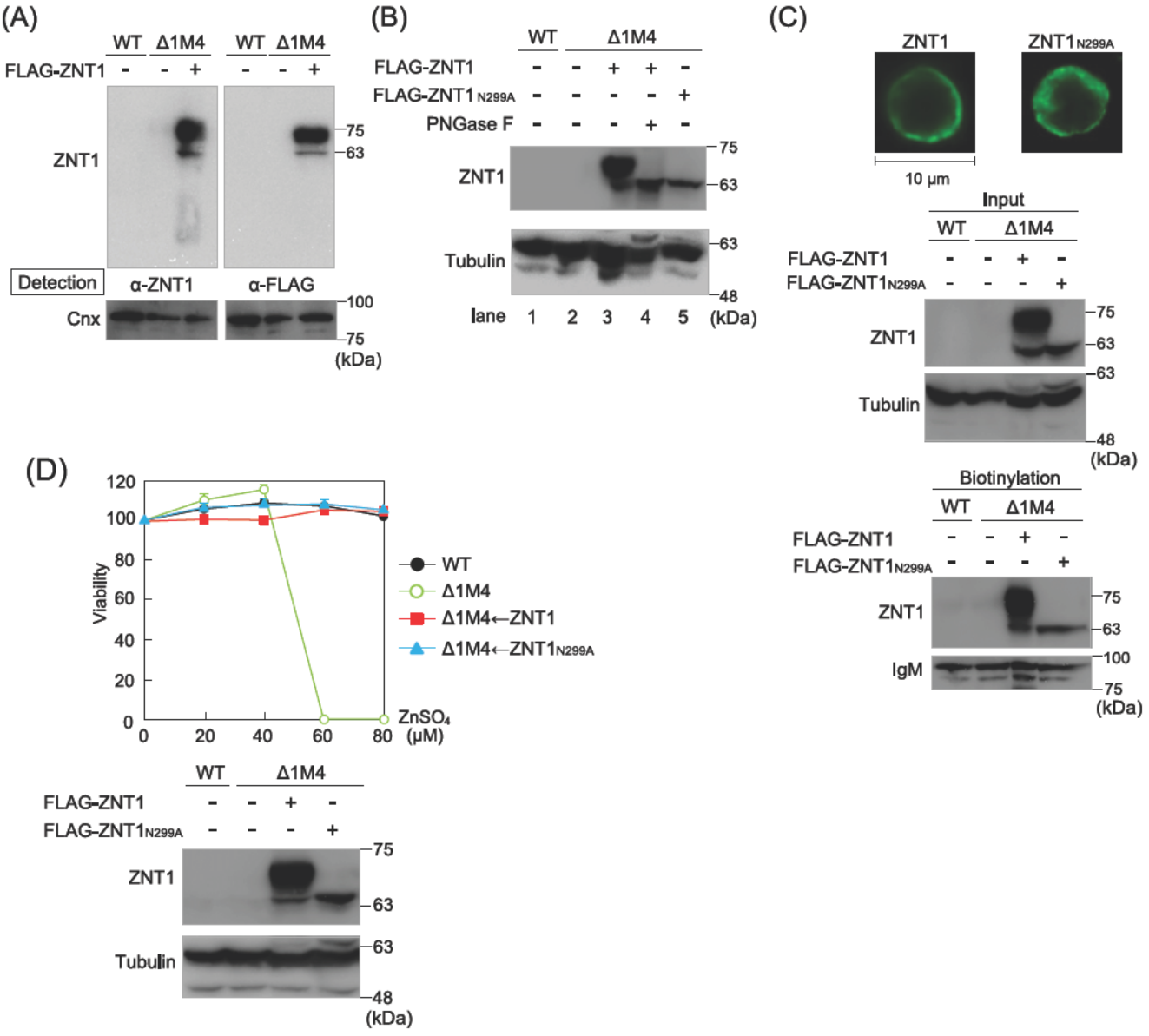

Figure 1. ZNT1 is *N*-glycosylated on the Asn^{299} residue of the extracellular loop between transmembrane domains V and VI. *A*, ZNT1 mAb specifically detected FLAG-ZNT1 protein expressed in *znt1*$^{-/-}$*mt*$^{-/-}$*znt4*$^{-/-}$ (Δ1M4) cells, as did anti-FLAG M2 antibody. *B*, ZNT1 is *N*-glycosylated at Asn^{299}. Total cell lysate prepared from Δ1M4 cells overexpressing ZNT1 was treated with (*lane 4*) or without (*lane 3*) PNGase F. Total cell lysate was also prepared from Δ1M4 cells overexpressing ZNT1$_{N299A}$ mutant (*lane 5*). Note that nonglycosylated ZNT1 proteins of the same size were detected in *lanes 4* and *5*. In *A* and *B*, calnexin (*Cnx*) and tubulin were used as loading controls, respectively. *C*, ZNT1$_{N299A}$ mutant located on the plasma membrane, as in wildtype (WT) ZNT1. Immunofluorescence staining confirmed that the ZNT1$_{N299A}$ mutant was located on the cell surface, as was WT ZNT1 (*upper two panels*). A cell surface biotinylation assay confirmed this (*other panels*). *Input* refers to aliquots of the biotinylated proteins before avidin capture (*i.e.* total cell lysate), and *biotinylation* refers to avidin-captured proteins. Tubulin and IgM were used as loading controls for input and biotinylation, respectively. *D*, ZNT1$_{N299A}$ mutant retained the ability to confer resistance against high zinc concentrations. WT DT40, Δ1M4, Δ1M4 cells overexpressing WT ZNT1, and Δ1M4 cells overexpressing ZNT1$_{N299A}$ were grown in the presence of the indicated concentrations of $ZnSO_4$ for 2 days, and the number of live cells was evaluated by an AlamarBlue® assay. Relative values are plotted as a percentage of live cells without $ZnSO_4$ for each group of cells. Each experiment was performed at least three times, and representative results are displayed.

and in response to increases in zinc concentration (Fig. 3*D*). MT expression increased with that of ZNT1, but was higher than that of ZNT1 (Fig. 3, *C* and *D*). Similar responses of both proteins were confirmed in PANC1 cells (Fig. 3, *E* and *F*). Therefore, ZNT1 protein expression as well as mRNA expression (23, 25, 30), increases in response to an increase in zinc concentration. The cell surface biotinylation assay of HepG2 cells revealed that ZNT1 accumulation on the plasma membrane increased in response to increased zinc (Fig. 3*G*), consistent with its zinc-efflux function.

We then examined the possibility that ZNT1 accumulation on the plasma membrane was directly facilitated by increased zinc, not just by increases in translation following its transcriptional up-regulation in response to increases in zinc. We used *mtf-1* knockout (*mtf-1* KO) MEF cells, because we assumed that the effects of zinc on ZNT1 cell surface accumulation are directly evaluated in *mtf-1* KO MEF cells, which have lost cellular responses to high zinc toxicity through up-regulating the transcription of a set of zinc-responsive genes, such as *MT* and *ZNT1* (31, 32). Culturing in high zinc concentrations (80 μM

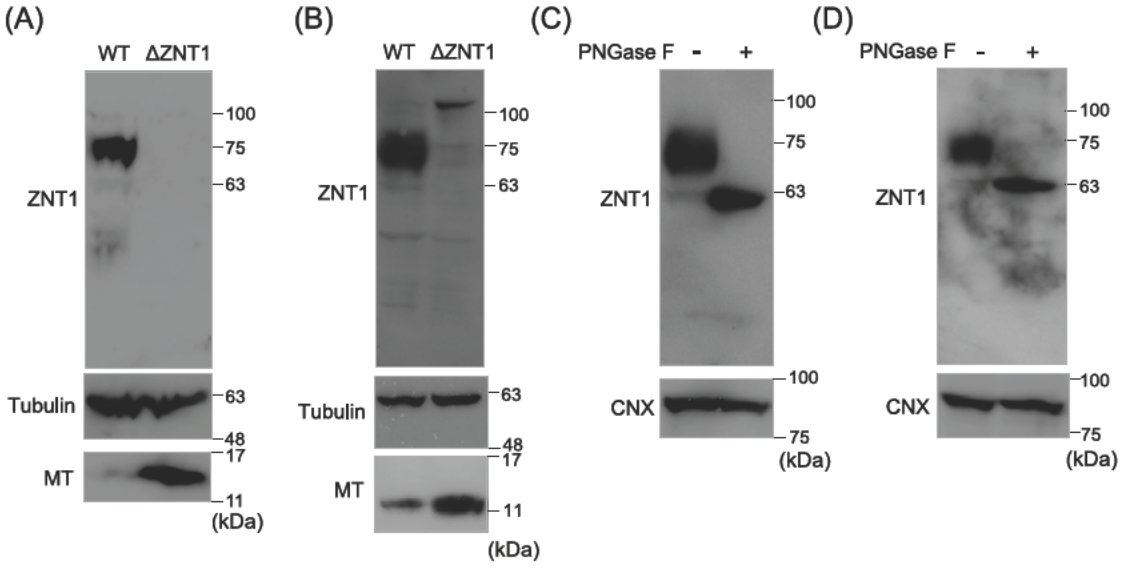

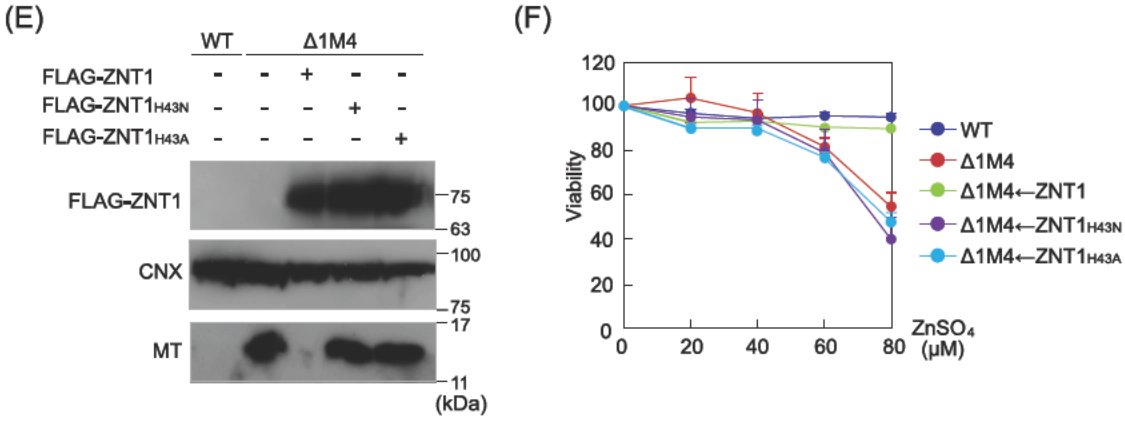

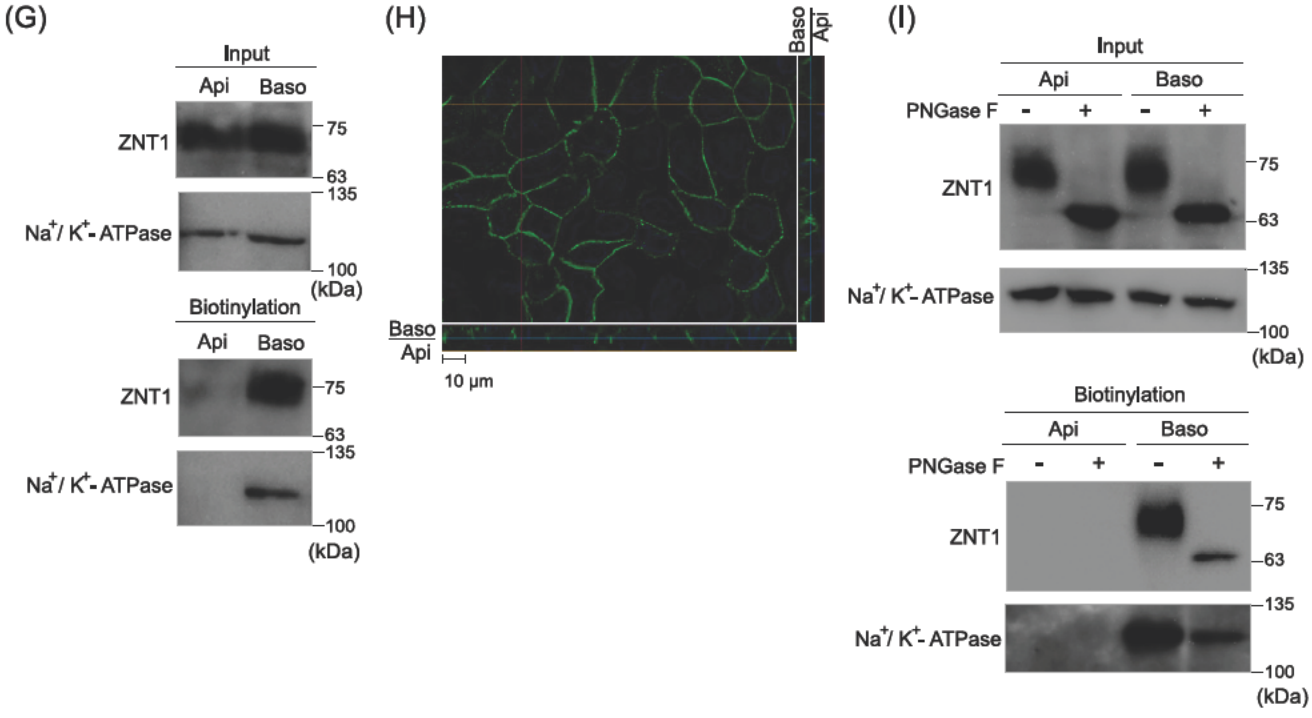

$ZnSO_4$ or higher concentrations) significantly decreased the viability of *mtf-1* KO MEF cells, which was reversed by constitutive ZNT1 expression (Fig. 3*H*). We then examined whether the accumulation of ZNT1 to the plasma membrane was facilitated by treating the cells with 20 μM $ZnSO_4$ after culture in zinc-deficient medium for 48 h to remove accumulated ZNT1 from the plasma membrane. Although the total ZNT1 protein expression level did not change in response to $ZnSO_4$ treatment (Fig. 3*I*, *input*), the cell surface ZNT1 protein expression level increased after 3 and 6 h (Fig. 3*I*, *biotinylation*), clearly indicating the facilitated accumulation of ZNT1 on the cell surface in response to increases in zinc.

ZNT1 accumulated on the cell surface is endocytosed and degraded in the proteasomal or lysosomal pathways under zinc deficiency

While performing the experiments described above, we found that cell surface ZNT1 levels decreased under zinc deficiency. Specifically, ZNT1 expression decreased for up to 48 h of zinc deficiency (Fig. 4*A*), and the decrease was restored by zinc supplementation in HepG2 cells (Fig. 4*B*). Similar changes in ZNT1 expression were observed in PANC1 cells (Fig. 4, *C* and *D*). The decreases in ZNT1 expression were in concert with those of the MT protein, although MT responses were greater (Fig. 4, *A–D*). We then explored whether cell surface ZNT1 expression was directly affected by zinc deficiency. ZNT1 expression on the cell surface decreased according to both a cell surface biotinylation assay (Fig. 4*E*) and immunofluorescence microscopy (Fig. 4*F*) in zinc-deficient culture for up to 48 h. *ZNT1* mRNA expression was almost constant (Fig. 4*H*), whereas ZNT1 protein expression significantly decreased during zinc deficiency (Fig. 4*G*).

We then conducted a time course experiment in which ZNT1 degradation was monitored after protein synthesis was blocked by cycloheximide (CHX). ZNT1 degradation was only detected by treating HepG2 cells with CHX (Fig. 4*I*, *lanes 2–4*). The degradation rate of the ZNT1 protein was increased under zinc deficiency, which was caused by treatment with the membrane-permeable zinc chelator TPEN (Fig. 4*I*, *lanes 5–7*), which was suppressed by 20 μM $ZnSO_4$ supplementation (Fig. 4*I*, *lanes 8–10*), indicating that physiological levels of zinc inhibit ZNT1 protein degradation. We then examined the effects of lysosome and proteasome inhibitors on ZNT1 degradation. Treatment with TPEN reduced ZNT1 protein expression levels, which were restored by treatment with the proteasomal inhibitor MG132 or lysosomal inhibitor bafilomycin A1 (Fig. 4*J*, *upper* panel), indicating that ZNT1 is degraded in both cellular degradation pathways during zinc deficiency. In this experiment, MG132 and BafA1 restored ZNT1 expression, but not the amount of ZNT1 on the cell surface (Fig. 4*J*, *lower* panel), suggesting that the ZNT1 that accumulates on the cell surface is endocytosed and then degraded. This is indeed the case, because blocking endocytosis by culturing the cells in a medium containing 350 mM sucrose suppressed ZNT1 protein degradation in both total cellular lysates and cell surface proteins (Fig. 4*K*). These results suggest that the ZNT1 protein expression level is controlled in a sophisticated manner to minimize zinc efflux from cells under zinc defeciency.

N-Glycosylation at Asn^{299} is involved in ZNT1 degradation

The above results indicate that ZNT1 protein expression is controlled in various ways. Because one of the unique features of ZNT1 is its *N*-glycosylation (see Fig. 1), we next examined whether or not it contributes to the regulation of ZNT1 protein expression by zinc status. We used MDCK FLp-In T-Rex (hereafter MDCK) cells stably expressing WT ZNT1 or the $ZNT1_{N299A}$ mutant to keep their protein expression levels comparable, because transcription was driven by a Tet-regulatable promoter from the same locus in cells harboring the FLp-In T-Rex system (Fig. 5*A*). First, to monitor the stability of WT ZNT1 and $ZNT1_{N299A}$ mutant proteins, the cells were cultured with doxycycline (Dox) for 24 h to induce ZNT1 expression, and then cultured for up to 6 h in the presence of CHX to block protein synthesis after Dox was washed out. No significant differences were observed in $ZNT1_{N299A}$ mutant expression during the time course, whereas marked decreases were found in WT ZNT1 protein expression (Fig. 5*B*, *input*). The protein degradation of WT ZNT1 increased in a zinc-deficient culture (Fig. 5*C*, *input*), and the cell surface biotinylation assay revealed that ZNT1 on the cell surface decreased in both conditions (Fig. 5, *B* and *C*, *biotinylation*), and significantly decreased under zinc deficiency. These results indicate that *N*-glycosylation at Asn^{299} is involved in ZNT1 degradation and its sensitivity to zinc deficiency.

Discussion

ZNT1 was the first identified mammalian zinc transporter (4). In contrast to its contribution to physiology and pathogenesis (10, 19, 22), its molecular expression regulation by zinc status has been poorly elucidated, except for its zinc-dependent transcription (23–25, 30). In this study, the clear detection of endogenous ZNT1 by our mAb enabled us to molecularly characterize it, and our findings are summarized as follows. First, ZNT1 protein accumulation on the cell surface increases in

Figure 2. Characterization of endogenous ZNT1 protein in cultured human cells. *A* and *B*, generation of *ZNT1*-deficient HAP1 (*A*) and PANC1 (*B*) cells. Genome editing was confirmed by genomic DNA sequencing (Fig. S1). In *A* and *B*, note that MT expression was significantly increased in *ZNT1*-deficient cells compared with WT cells. *C* and *D*, endogenous ZNT1 is *N*-linked glycosylated in HAP1 (*C*) and PANC1 (*D*) cells. Total cellular lysate prepared from cells were treated with or without PNGase F and then subjected to immunoblotting. *E*, re-expression of WT ZNT1, but not $ZNT1_{H43N}$ or $ZNT1_{H43A}$ mutants, restored the decreased MT expression in *ZNT1*-deficient PANC1 cells. *F*, reduced resistance to high zinc in *ZNT1*-deficient PANC1 cells was restored by WT ZNT1, but not $ZNT1_{H43N}$ or $ZNT1_{H43A}$ mutants. An AlamarBlue® assay was performed as shown in Fig. 1*D*. Relative values are plotted as a percentage of live cells without $ZnSO_4$ for each group of cells. *G* and *H*, endogenous ZNT1 was on the basolateral membrane in polarized CaCo2 cells. CaCo2 cells that were grown on Transwell® plates until polarized were subjected to cell surface biotinylation assays (*G*) or immunofluorescence staining with Z-stack analysis (*H*). *I*, ZNT1 on the basolateral membrane in polarized CaCo2 cells was *N*-glycosylated. Polarized CaCo2 cells were subjected to cell surface biotinylation assays, and biotinylated proteins were treated with or without PNGase F for 24 h before avidin capture. In *G* and *I*, *input* refers to aliquots of the biotinylated proteins before avidin capture, and *biotinylation* refers to avidin-captured proteins. Na^+/K^+-ATPase was used as a loading control for input and biotinylation. Each experiment was performed at least three times, and representative results are displayed.

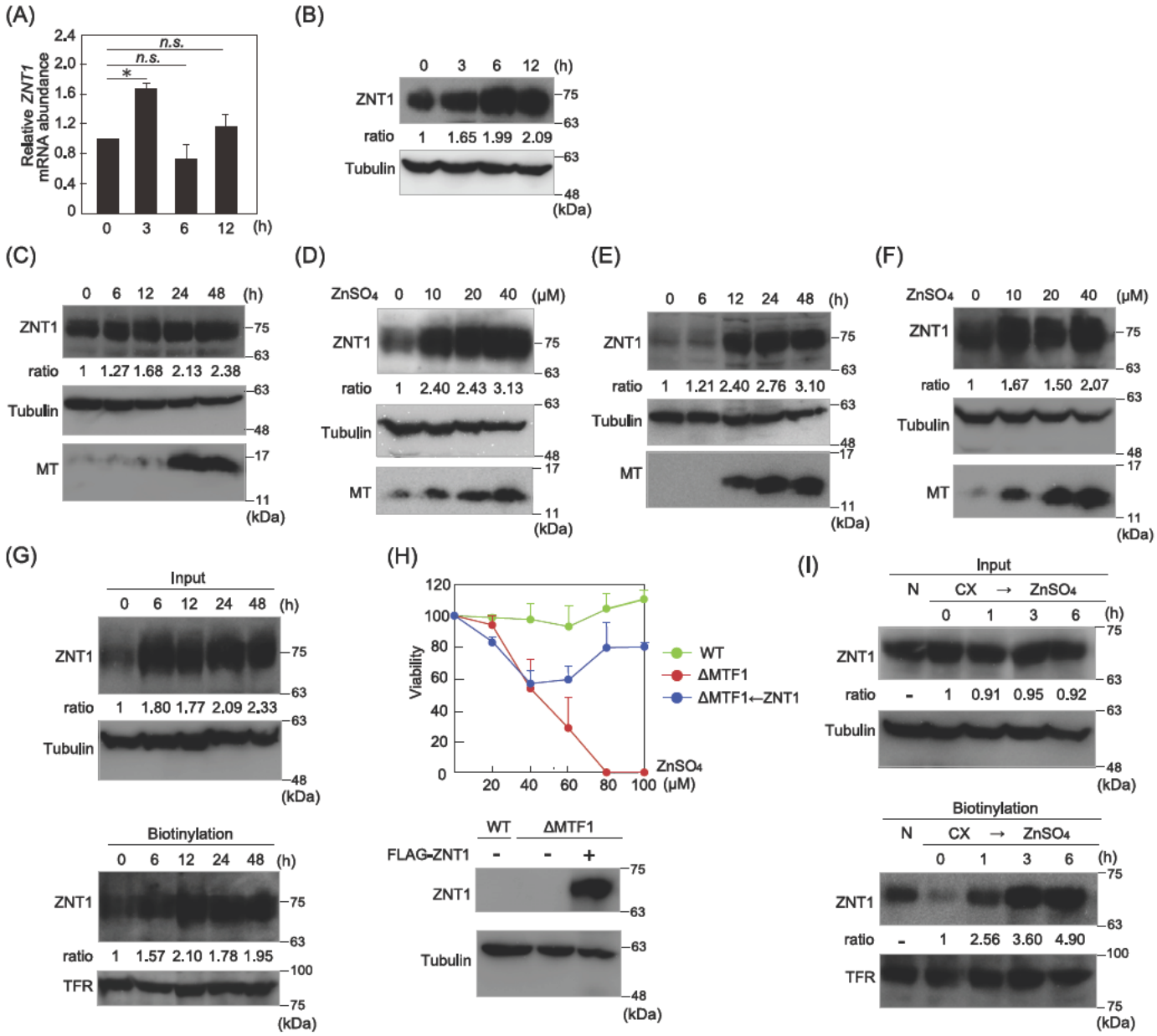

Figure 3. Zinc-induced cell surface expression of ZNT1 is enhanced by its facilitated accumulation. *A* and *B*, time course of *ZNT1* mRNA (*A*) and ZNT1 protein (*B*) expression in HepG2 cells treated with 50 μM $ZnSO_4$. In *A*, total RNA prepared from HepG2 cells was subjected to RT-qPCR. Changes in mRNA expression relative to that in a normal medium are shown after normalization with *Cyclophilin A* mRNA expression. Each value is the mean ± S.D. of three independent experiments (*, $p < 0.05$; *n.s.*, not significant). In *B*, changes in ZNT1 protein expression were evaluated by immunoblotting. *C–F*, zinc-induced expression of ZNT1 protein in HepG2 (*C* and *D*) and PNAC1 (*E* and *F*) cells. In *C and E*, both cells were cultured in medium supplemented with 20 μM $ZnSO_4$ for the indicated period, and in *D* and *F*, cells were cultured in a medium supplemented with the indicated concentration of $ZnSO_4$ for 48 h. In *C–F*, tubulin is shown as a loading control. *G*, zinc-induced ZNT1 accumulation on the cell surface. HepG2 cells were cultured in the same manner as shown in *C*, and cell surface biotinylation assays were performed. Tubulin and transferrin receptor (*TFR*) were used as loading controls for input and biotinylation, respectively. *H*, WT ZNT1 expression reversed the zinc-sensitive phenotypes of *mtf-1* KO MEF cells, which failed to grow in the presence of 80 μM $ZnSO_4$ or higher concentrations. *I*, ZNT1 protein displayed facilitated accumulation on the plasma membrane in response to increases in zinc. *mtf-1* KO MEF cells were cultured in zinc-deficient medium for 48 h and then cultured for the indicated time after 20 μM $ZnSO_4$ was added. The cell surface localization of the ZNT1 protein was evaluated by a cell surface biotinylation assay. Tubulin and TFR were used as loading controls for input and biotinylation, respectively. In *B–G* and *I*, the band intensities of ZNT1 were quantified by densitometric analysis after normalization to the levels of tubulin or TFR, and the ratio relative to the basal condition, which was set to 1.0, is shown *below* each lane. Each experiment was performed at least three times, and representative results are displayed.

response to increases in zinc, which is enhanced by its facilitated accumulation, in addition to transcriptional up-regulation. Second, the ZNT1 accumulated on the cell surface decreases because of degradation in cellular degradation pathways following endocytosis from the cell surface under zinc deficiency. Third, ZNT1 is *N*-glycosylated at Asn^{299} in the EL3 between transmembrane domains V and VI, which is important for its stabilization regulation, despite not affecting ZNT1's ability to traffic to the cell surface nor to confer cellular resistance against high zinc levels. This molecular evidence provides insights into ZNT1 protein functions, considering its multifarious physiological and pathological roles.

ZNT1 mRNA levels increase in response to excess zinc, which is mediated by the binding of MTF-1 to metal-response

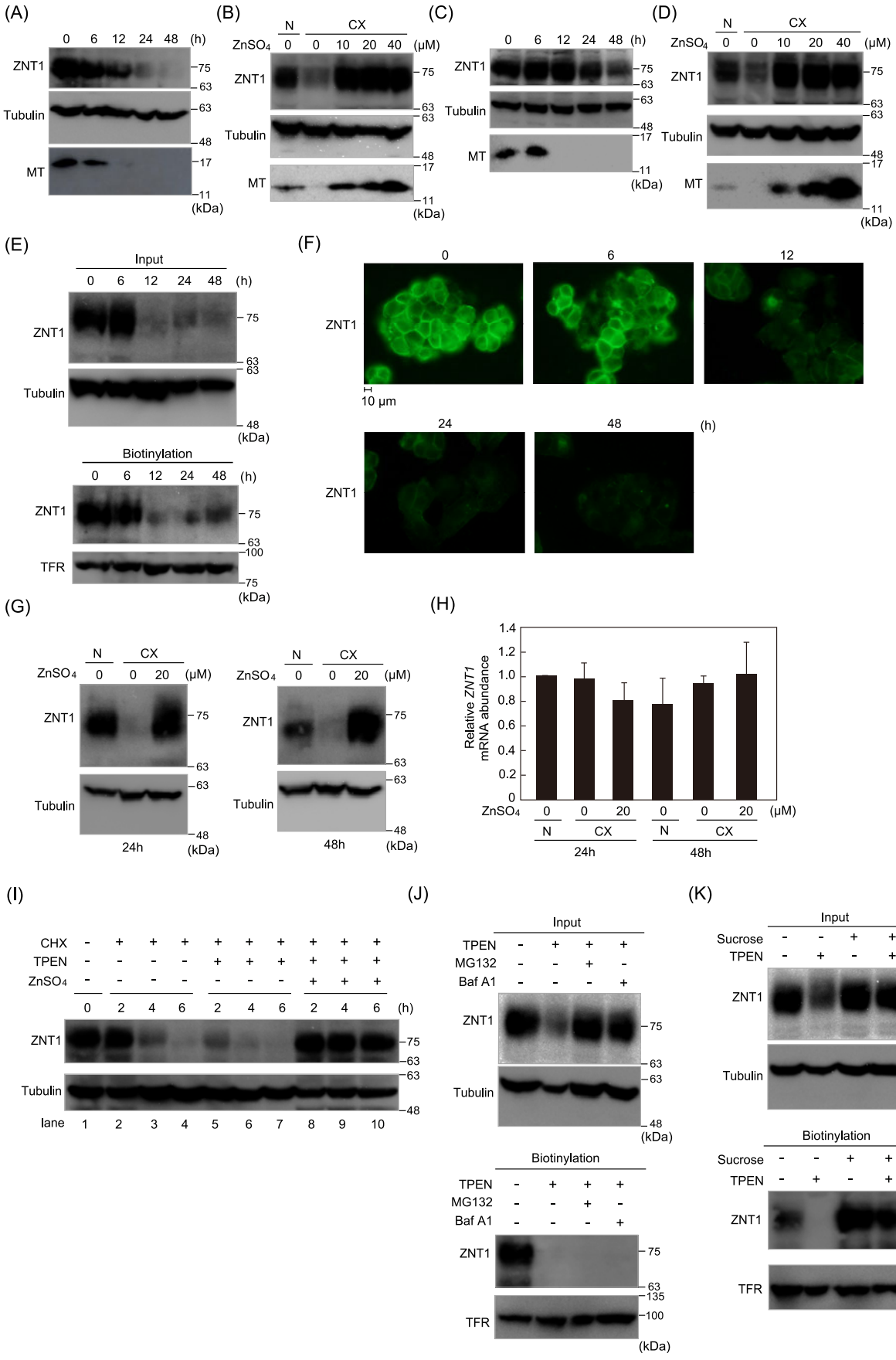

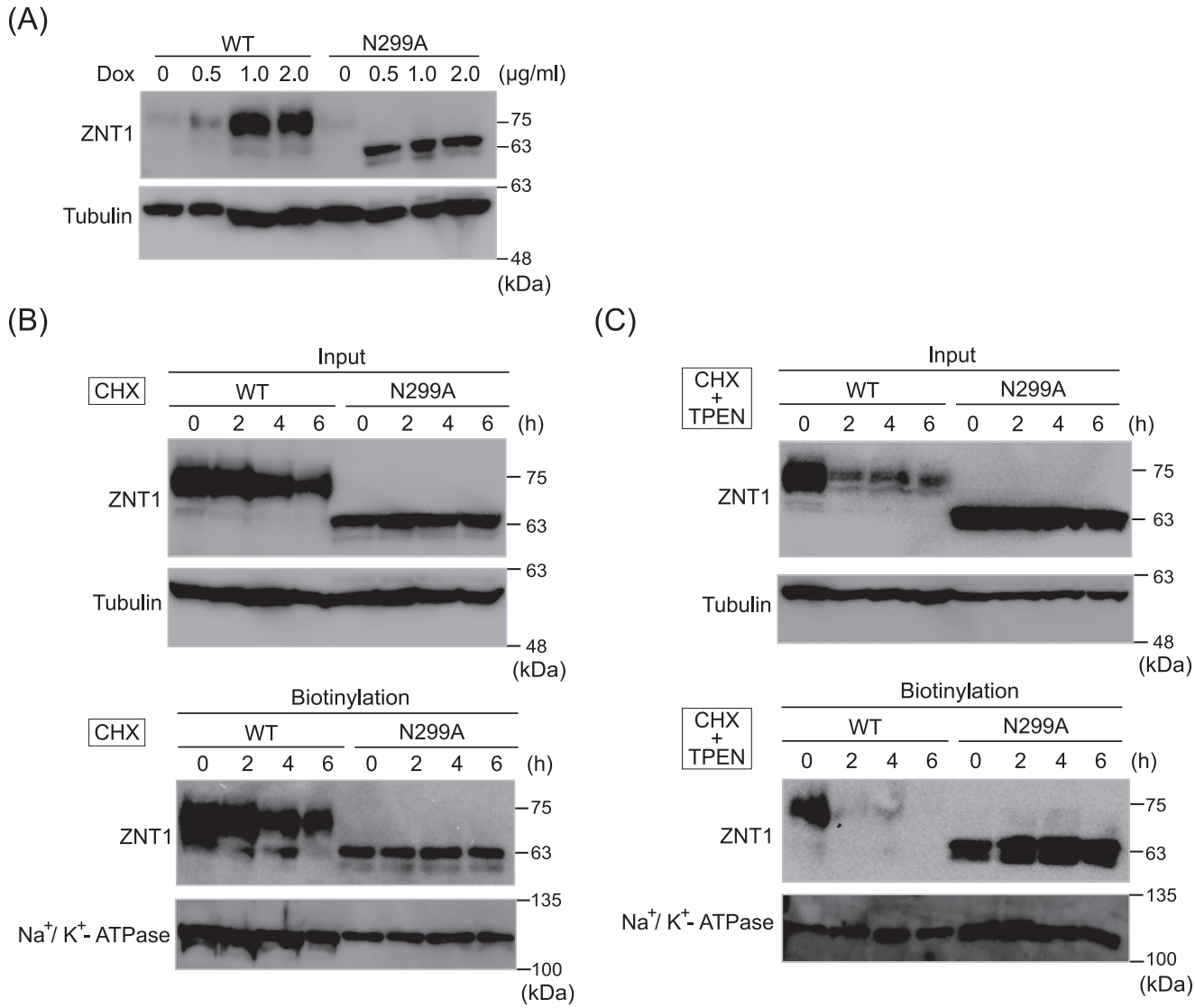

Figure 5. *N*-Glycosylation at Asn^{299} is involved in ZNT1 degradation. *A*, Dox-dependent expression of WT ZNT1 and ZNT1$_{N299A}$ mutant in MDCK FLp-In T-Rex (MDCK) cells. MDCK cells stably expressing WT ZNT1 and ZNT1$_{N299A}$ mutant were incubated with the indicated concentrations of Dox for 24 h. *B*, ZNT1$_{N299A}$ mutant was more stable than WT ZNT1 on the cell surface. MDCK cells expressing WT ZNT1 or ZNT1$_{N299A}$ mutant were treated with 20 μg/ml of CHX for 2, 4, or 6 h after treatment with 1.0 μg/ml of Dox for 24 h, and cell surface biotinylation assays were performed as described in the legend to Fig. 1C. *C*, zinc deficiency facilitated the degradation of WT ZNT1 on the cell surface. MDCK cells were cultured as in *B*, except for adding zinc chelator TPEN, and subjected to the same experiments. In *B* and *C*, tubulin and Na^+/K^+-ATPase were used as loading controls for input and biotinylation, respectively. Each experiment was performed at least three times, and representative results are displayed.

elements in *ZNT1*'s promoter (23–25). Because MT has a similar response, ZNT1 and MT may cooperatively manage cellular responses against zinc toxicity (13). To perform this function efficiently, ZNT1 has been speculated to accumulate on the cell surface (33); however, this idea has not been proven experimentally. We show that ZNT1 protein accumulation on the

Figure 4. ZNT1 accumulated on the cell surface is endocytosed and degraded in the proteasomal or lysosomal pathways during zinc deficiency. *A*, zinc deficiency deceased ZNT1 protein levels in HepG2 cells. Cells were cultured in a zinc-deficient medium containing fetal calf serum treated with Chelex 100 resin (*CX*) for the indicated period. *B*, zinc supplementation into the CX medium restored ZNT1 protein expression in HepG2 cells. Cells were cultured in normal medium (*N*), zinc-deficient medium (*CX*), or CX medium supplemented with the indicated concentration of $ZnSO_4$ for 48 h. *C* and *D*, zinc deficiency deceased ZNT1 protein levels, which were restored by zinc supplementation in PANC1 cells, as is HepG2 cells. In *A–D*, ZNT1 levels were analyzed by immunoblotting. Note that MT expression was significantly decreased in zinc-deficient cultures. Tubulin is shown as a loading control. *E* and *F*, ZNT1 protein disappeared on the plasma membrane during zinc deficiency. HepG2 cells were cultured in a zinc-deficient medium (*CX*) for the indicated period, and cell surface biotinylation assays (*E*) or immunofluorescence staining (*F*) were performed. *G* and *H*, comparison of ZNT1 protein expression levels in HepG2 cells cultured in normal medium (*N*), zinc-deficient medium (*CX*), or CX supplemented with 20 μM $ZnSO_4$ for 24 or 48 h (*G*), and *ZNT1* mRNA expression levels in HepG2 cells cultured under the same conditions (*H*). The differences were not statistically significant. *I*, physiologically relevant levels of zinc inhibited ZNT1 protein degradation. HepG2 cells were cultured in the presence of 20 μg/ml of CHX, 20 μg/ml of CHX with 25 μM TPEN, and 20 μg/ml of CHX with 25 μM TPEN supplemented with 20 μM $ZnSO_4$ for 2, 4, or 6 h. Immunoblotting was performed as described above. *J*, degradation of ZNT1 triggered by zinc deficiency required both proteasomal and lysosomal degradation pathways. HepG2 cells were treated with 20 μg/ml of CHX, and 10 μM MG132 (proteasome inhibitor), or 10 nM Bafilomycin A1 (lysosome inhibitor) was added for 2 h. Cells were then treated with 25 μM TPEN (zinc chelator) for 6 h, and cell surface biotinylation assays were performed. *K*, zinc deficiency stimulated the endocytosis of the ZNT1 protein before its degradation. HepG2 cells were treated with 350 mM sucrose for 2 h followed by 25 μM TPEN for 6 h. Cell surface biotinylation assays were performed. Each experiment was performed at least three times, and representative results are displayed.

Table 1

Conservation of the *N*-glycosylation site in extracellular loop 3 (EL3) among ZNT1 orthologs

Sequences corresponding to EL3 between transmembrane domains V and VI are aligned as previously described (56). The following are accession numbers of the sequences used: *Homo sapiens*, NP_067017.2; *Mus musculus*, NP_033605.1; *Canis lupus familiaris*, XP_003434978.3; *Gallus gallus*, BBM28213.1; *Danio rerio*, NP_957173.1; *C. elegans*, NP_509095.1; *Drosophila melanogaster*, NP_647801.1. The potential *N*-glycosylation site is indicated in bold.

Ortholog	Amino acid sequence	Species
ZNT1	^{259}SVIVVVNALVFYFSWKGCSEGDFCVNPCFPDPCKAFVEII**NST**HASVYEAGPCWVLYLD^{317}	*Homo sapiens*
Znt1	^{254}SVIVVVNALVFYFNWKGCTEDDFCTNPCFPDPCKSSVEII**NST**QAPMRDAGPCWVLYLD^{312}	*Mus musculus*
Znt1	^{244}SVIVVVNALVFYFSWRGCPEGEFCVNPCIPDPCKAFVEII**NST**HATVHEAGPCWVLYLD^{302}	*Canis lupus familiaris*
Znt1	^{261}SVIVVVNALLFYGLWNPCPKDGPCFNPCVNSHCVE**NAT**LSQPLGSANKSEQESITVAGPCWLLYLD^{326}	*Gallus gallus*
Znt1	^{247}SVIVVINAIIFVFVWKPCEPGTICENPCSGQHCADHAL**NIS**SPLTNGTLIKAGPCWVLYLD^{307}	*Danio rerio*
Cdf-1	^{357}SVIVMISAGFVYFL----------PTWKIAAYLD^{380}	*Caenorhabditis elegans*
Znt63C	^{211}SIIVVISAVVVWKTEWK----------YRYYMD^{233}	*Drosophila melanogaster*

cell surface is not only increased by its expression, but also by its facilitated accumulation to the plasma membrane in response to increases in zinc. This novel response is important, because it enables a rapid response to high zinc levels without requiring transcription. The cell surface accumulation of ZNT1 is reminiscent of the copper efflux transporter ATP7A, which accumulates on the plasma membrane from the *trans*-Golgi network to export copper under high copper conditions (34, 35). Phosphorylation is important in the trafficking of ATP7A (36, 37). Because ZNT1 has a potential phosphorylation site at Ser^{506} in the cytosolic C-terminal (38), similar phosphorylation mechanisms may regulate ZNT1 accumulation. In addition, the facilitated cell surface accumulation of ZNT1 is reminiscent of the cell surface expression of ZIP4, although it responds to zinc in the opposite manner. ZIP4 accumulates on the cell surface through reduced internalization from the plasma membrane during zinc deficiency and is rapidly degraded via endocytosis in response to excess zinc (39, 40), but the molecular mechanism behind this has not yet been elucidated. Further investigation is required to elucidate the molecular regulation events underlying the facilitated accumulation of ZIP4 and ZNT1 on the cell surface.

Another significant result of this study is that we found that ZNT1 was degraded via both proteasomal and lysosomal pathways under zinc deficiency. Zinc deficiency triggers endocytosis of cell surface ZNT1, leading to lysosomal degradation, and also potentially the degradation of nascent and intracellular localized ZNT1, through proteasomal degradation via the endoplasmic reticulum-associated protein degradation (ERAD) pathway. This novel response of ZNT1 would be physiologically important for minimizing the zinc efflux from cells during zinc deficiency because it was observed in cells that were made zinc-deficient in a physiologically relevant manner using Chelex 100-treated fetal calf serum (FCS). Importantly, the degradation of ZNT1 was in concert with that of MT. Considering the concerted degradation of ZNT1 and MT under zinc deficiency, their expression regulation should ensure the use of cytoplasmic zinc in cells during such conditions, and thus be critical for homeostasis maintenance.

As mentioned in the Introduction, ZNT1 is a moonlighting protein. It plays pivotal roles as a zinc exporter on the cell surface and as a binding partner for several proteins in the ER, and operates as a scaffold protein. Our results highlight the zinc-responsive accumulation of ZNT1, which would improve our understanding of the moonlighting functions of ZNT1, *e.g.* ZNT1 accumulation on the cell surface in response to cellular zinc increases may reduce its scaffold functions. Zinc-responsive expression regulation of ZNT1 may be a novel mechanism of zinc signaling control, considering the important functions of its binding partner proteins, such as RAF-1 and calcium channels. This attractive hypothesis needs further investigation.

For the first time, we present evidence that ZNT1 is *N*-glycosylated at Asn^{299}, and this is involved in stability control but not in zinc efflux functions, as well as its cell surface localization. In a previous study, ZNT2 was shown to be *N*-glycosylated (41), but its biological significance has not yet been clarified. Therefore, our finding is novel and interesting, in that one can consider the role of extracellular glycosylation in cellular zinc homeostasis. The *N*-glycosylation site of ZNT1 is conserved among its vertebrate orthologs, but not in the nematode or fruit fly (Table 1). Therefore, fine-tuned ZNT1 expression regulation mediated by *N*-glycosylation may have only been acquired in vertebrates. The *N*-glycosylation of metal transporters may be important as a regulatory mechanism for maintaining metal homeostasis, *e.g.* the glycosylation of ZIP14 is crucial for its degradation control and its sensitivity to iron, so its deglycosylation results in its stabilization (42), as in the case of ZNT1. Similar mechanisms may operate in the degradation control of these two metal transporters. Further investigation is required to clarify this point.

We found that ZNT1 expression on the cell surface is increased by treatment with 20 μM $ZnSO_4$, and its degradation can be blocked by normal culture medium. These zinc concentrations are physiologically relevant. Moreover, cell surface-accumulated ZNT1 protein was degraded in a zinc-deficient culture containing Chelex-treated FCS, which is the same condition that facilitated ZIP4 protein accumulation in our previous studies (39, 40, 43, 44). Therefore, zinc-responsive ZNT1 protein expression is probably physiologically significant. The regulation of ZNT1 expression on the cell surface is reciprocal to that of ZIP4. Moreover, ZIP4 is located on the apical membrane of enterocytes and takes zinc up from the intestinal lumen (45–49), whereas ZNT1 is located on the basolateral membrane in enterocytes and exports zinc into the bloodstream (6, 10, 20). We confirmed that the ZNT1 protein located on the basolateral membrane of CaCo2 cells is *N*-glycosylated (see Fig. 2*I*), which is required for fine-tuned regulation; therefore, ZNT1 expression could be controlled in a sophisticated manner in enterocytes. Reciprocal expression of ZNT1 and ZIP4 in enterocytes would contribute to zinc absorption regulation (50).

In conclusion, the results of this study dissect the molecular properties of ZNT1, and indicate that cellular and systemic zinc homeostasis is sophisticatedly maintained by the dynamic regulation of ZNT1 expression in multiple manners, although fur-

ther studies are required to elucidate the physiological and pathological significance of ZNT1 expression regulation. Zinc entry into the cells is carried out by numerous ZIP proteins, whereas the zinc efflux pathway is mostly mediated by only ZNT1. Thus, the present study provides the molecular basis to understand homeostatic control of zinc.

Experimental procedures

Cell culture

Chicken B lymphocyte-derived DT40 cells were maintained in RPMI 1640 (Nacalai Tesque, Kyoto, Japan) supplemented with 10% (v/v) heat-inactivated FCS (Sigma), 1% (v/v) chicken serum (Invitrogen), 50 μM 2-mercaptoethanol (Sigma), 100 units of penicillin/ml, and 100 μg of streptomycin/ml at 39.5 °C, as previously described (26). Human myelogenous leukemia HAP1 (Horizon Discovery, Cambridge, UK) cells were maintained in Iscove's modified Dulbecco's medium (Nacalai Tesque) containing 10% (v/v) heat-inactivated FCS (Sigma), 100 units of penicillin/ml, and 100 μg of streptomycin/ml at 37 °C. HepG2 or MDCK FLp-In T-Rex (51) and CaCo2 or *mtf-1* KO MEF (24) cells were maintained in Dulbecco's modified Eagle's medium (Sigma) containing 10% (v/v) heat-inactivated FCS, 100 units of penicillin/ml, and 100 μg of streptomycin/ml at 37 °C. Rather than Dulbecco's modified Eagle's medium, RPMI 1640 medium was used to maintain the PANC1 cells. Caco2 cells were cultured for 3 weeks on 24-mm polyester-membrane Transwell® plates with 0.4-μm pores (Greiner Bio-One) to allow the formation of tight junctions. To generate a zinc-deficient culture medium, FCS was treated with Chelex 100 resin as described previously (52). Proteasome inhibitor MG132 (Peptide Institute Inc.) or lysosome inhibitor bafilomycin A1 (Sigma) was used to block protein degradation at the indicated final concentrations in the figure legends.

Plasmid construction

Plasmids used to express N-terminally FLAG-tagged ZNT1 (both WT and mutants) were constructed by inserting each cDNA into a pA-Puro vector as described previously (26). Substitution mutants were constructed by two-step polymerase chain reaction (PCR) methods. All plasmids were linearized with appropriate restriction enzymes prior to electroporation for DT40 cells or lipofection using Lipofectamine 2000 reagent (Invitrogen) for other cells used in this study, to establish stable transfectants.

Disruption of ZNT1 genes in HAP1 and PANC1 cells

ZNT1-knockout cells were generated using the CRISPR/Cas9 system. Guide RNA expression plasmids were generated by inserting the following oligonucleotides into the BbsI or BsaI site of a PX-330-B/B vector (53): *ZNT1-F*, 5′-CACCGGATCCGAGCCGAGGTAATG-3′; *ZNT1-R*, 5′-AAACCATTACCTCGGCTCGGATCC-3′. The constructed plasmids were cotransfected with pcDNA6/TR, which contained a blasticidin resistance gene, or pA-Neo, which contained a neomycin resistance gene, into HAP1 or PANC1 cells using Lipofectamine 2000 reagent. The cells were cultured with 20 μg/ml of blasticidin (InvivoGen) or 600 μg/ml of G418 sulfate (Nacalai Tesque) to generate stable clones. HAP1 or PANC1 cells deficient in the *ZNT1* gene were confirmed by directly sequencing the PCR-amplified fragments using genomic DNA as a template (Table S1 and Fig. S1).

Immunoblotting

Immunoblotting was performed as described previously (54). Briefly, a blotted polyvinylidene difluoride membrane (Immobilon-P, Millipore Corp., Bedford, MA) was blocked with 5% skimmed milk and 0.1% Tween 20 in PBS prior to incubation with anti-FLAG M2 (1:3,000; F3165, Sigma), anti-ZNT1 (1:3,000) (26), anti-MT (1:3000, clone E9; Dako, Carpinteria, CA), anti-calnexin (1:10,000; ADI-SPA-860, Enzo Life Sciences), anti-Na^+/K^+-ATPase (1:500; catalog number sc-28800, Santa Cruz Biochemistry, Santa Cruz, CA), and anti-α-tubulin (1:10,000; Developmental Studies Hybridoma Bank (DSHB) by J. Frankel and E. M. Nelsen) antibodies in blocking solution. Horseradish peroxidase-conjugated anti-mouse or anti-rabbit secondary antibodies (GE Healthcare, NA931 or NA934) were added at a 1:3,000 dilution for detection. A fluoroimage was obtained using a LAS500 (GE Healthcare). Densitometric quantification of band intensity was performed using ImageQuant TL software (GE Healthcare).

Cell surface biotinylation assay

Cell surface biotinylation assay was performed as described previously (26, 43). Cells were washed with ice-cold PBS, and then EZ-Link, a sulfo-NHS-SS-biotin reagent (Pierce Protein Biology, Thermo Fisher Scientific, Rockford, IL), was added to biotinylate lysine residues exposed on the extracellular surface. Biotinylated proteins were recovered from streptavidin-coupled beads in 6× SDS sample buffer and then immunoblotted.

PNGase F digestion

Digestion of *N*-glycosylation was performed using PNGase F (New England Biolabs, Beverly, MA). Briefly, total cell lysates were denatured with denaturing buffer (0.5% SDS, 40 mM DTT) at 37 °C for 30 min and digested with PNGase F in the reaction buffer (50 mM sodium phosphate, 1% Nonidet P-40) for 2 h at 37 °C. Each sample was mixed with 6× SDS sample buffer and then subjected to immunoblotting. Digestion of a biotinylated membrane prepared from CaCo2 cells was performed in the presence of a protease inhibitor mixture (Nacalai Tesque) for 24 h at 37 °C after denaturation.

Immunofluorescence staining

Immunostaining for the detection of ZNT1 was performed as previously described (26). Briefly, cells were fixed with 10% formaldehyde neutral buffer solution (Nacalai Tesque) and stained with anti-ZNT1 (1:1,000 dilution) followed by Alexa 488-conjugated goat anti-mouse IgG (Molecular Probes, Eugene, OR) without permeabilization. The stained cells were observed using a FSX100 fluorescent microscope (Olympus, Tokyo, Japan), and images were analyzed using Adobe Photoshop CS. Z-stack images of the immunofluorescence microscopy were also taken using FSX100.

Cytotoxicity assay against high zinc concentrations

An AlamarBlue® assay was performed as previously described (26). DT40 cells were cultured at a density of 10×10^4 cells/ml in a 96-well plate and treated with $ZnSO_4$ at the indicated concentrations for 2 days. PANC-1 or *mtf-1* KO MEF cells were cultured at a density of 1.0×10^4 cells/ml in a 96-well plate and treated with $ZnSO_4$ at the indicated concentrations for 2 days. AlamarBlue® reagent was added to the medium, which was then incubated for 4 h. Absorbance was measured at 570 and 600 nm using PowerScan4.

Reverse transcription-quantitative PCR (RT-qPCR)

RT-qPCR was performed as described previously (43). Briefly, total RNA (1 μg) isolated from HepG2 cells was reverse-transcribed using ReverTra Ace (Toyobo, Osaka, Japan), and a real-time PCR was performed using a Thunderbird SYBR® qPCR Mix (Toyobo). Samples were denatured at 95 °C for 2 min and amplified for 40 reaction cycles with denaturation at 95 °C for 15 s, annealing at 57 °C for 15 s, and extension at 72 °C for 30 s per cycle. Each cDNA sample was prepared in triplicate, and the same reaction was performed without using reverse transcriptase as a negative control. *Cyclophilin A* was used to normalize each sample. Primer sequences for *ZNT1* and *Cyclophilin A* were designed as described elsewhere (55) (Table S2).

Statistical analyses

All data are presented as the mean ± S.D. Statistical significance was determined using Student's *t* test and accepted at $p < 0.05$.

Author contributions—Y. N. and T. K. conceptualization; Y. N. and T. K. resources; Y. N. and T. K. data curation; Y. N. software; Y. N. formal analysis; Y. N. and T. K. funding acquisition; Y. N. and T. K. validation; Y. N. and T. K. investigation; Y. N. and T. K. visualization; Y. N. and T. K. methodology; Y. N. and T. K. writing-original draft; Y. N. and T. K. project administration; Y. N. and T. K. writing-review and editing; T. K. supervision.

Acknowledgments—We thank Dr. Glen K. Andrews (University of Kansas Medical Center), Dr. Jack Kaplan (University of Illinois College of Medicine), and Dr. Shuichi Enomoto (Okayama University) for the gifts of mtf-1 KO MEF, MDCK FLp-In T-Rex, and PANC1 cells, respectively, Dr. Tomohiro Yamazaki (Hokkaido University) for experimental suggestions and supports, and Dr. Hiroyuki Yasui (Kyoto Pharmaceutical University) for the opportunity to perform the study.

References

1. Hara, T., Takeda, T. A., Takagishi, T., Fukue, K., Kambe, T., and Fukada, T. (2017) Physiological roles of zinc transporters: molecular and genetic importance in zinc homeostasis. *J. Physiol. Sci.* **67,** 283–301 CrossRef Medline
2. Kambe, T., Tsuji, T., Hashimoto, A., and Itsumura, N. (2015) The physiological, biochemical, and molecular roles of zinc transporters in zinc homeostasis and metabolism. *Physiol. Rev.* **95,** 749–784 CrossRef Medline
3. Lichten, L. A., and Cousins, R. J. (2009) Mammalian zinc transporters: nutritional and physiologic regulation. *Annu. Rev. Nutr.* **29,** 153–176 CrossRef Medline
4. Palmiter, R. D., and Findley, S. D. (1995) Cloning and functional characterization of a mammalian zinc transporter that confers resistance to zinc. *EMBO J.* **14,** 639–649 CrossRef Medline
5. McMahon, R. J., and Cousins, R. J. (1998) Regulation of the zinc transporter ZnT-1 by dietary zinc. *Proc. Natl. Acad. Sci. U.S.A.* **95,** 4841–4846 CrossRef Medline
6. Yu, Y. Y., Kirschke, C. P., and Huang, L. (2007) Immunohistochemical analysis of ZnT1, 4, 5, 6, and 7 in the mouse gastrointestinal tract. *J. Histochem. Cytochem.* **55,** 223–234 CrossRef Medline
7. Merriman, C., Huang, Q., Gu, W., Yu, L., and Fu, D. (2018) A subclass of serum anti-ZnT8 antibodies directed to the surface of live pancreatic beta-cells. *J. Biol. Chem.* **293,** 579–587 CrossRef Medline
8. Huang, Q., Merriman, C., Zhang, H., and Fu, D. (2017) Coupling of insulin secretion and display of a granule-resident zinc transporter ZnT8 on the surface of pancreatic beta cells. *J. Biol. Chem.* **292,** 4034–4043 CrossRef Medline
9. Henshall, S. M., Afar, D. E., Rasiah, K. K., Horvath, L. G., Gish, K., Caras, I., Ramakrishnan, V., Wong, M., Jeffry, U., Kench, J. G., Quinn, D. I., Turner, J. J., Delprado, W., Lee, C. S., Golovsky, D., *et al.* (2003) Expression of the zinc transporter ZnT4 is decreased in the progression from early prostate disease to invasive prostate cancer. *Oncogene* **22,** 6005–6012 CrossRef Medline
10. Cousins, R. J., Liuzzi, J. P., and Lichten, L. A. (2006) Mammalian zinc transport, trafficking, and signals. *J. Biol. Chem.* **281,** 24085–24089 CrossRef Medline
11. Palmiter, R. D., and Huang, L. (2004) Efflux and compartmentalization of zinc by members of the SLC30 family of solute carriers. *Pflugers Arch.* **447,** 744–751 CrossRef Medline
12. Nolte, C., Gore, A., Sekler, I., Kresse, W., Hershfinkel, M., Hoffmann, A., Kettenmann, H., and Moran, A. (2004) ZnT-1 expression in astroglial cells protects against zinc toxicity and slows the accumulation of intracellular zinc. *Glia* **48,** 145–155 CrossRef Medline
13. Palmiter, R. D. (2004) Protection against zinc toxicity by metallothionein and zinc transporter 1. *Proc. Natl. Acad. Sci. U.S.A.* **101,** 4918–4923 CrossRef Medline
14. Tsuda, M., Imaizumi, K., Katayama, T., Kitagawa, K., Wanaka, A., Tohyama, M., and Takagi, T. (1997) Expression of zinc transporter gene, ZnT-1, is induced after transient forebrain ischemia in the gerbil. *J. Neurosci.* **17,** 6678–6684 CrossRef Medline
15. Sindreu, C., Bayés, Á., Altafaj, X., and Pérez-Clausell, J. (2014) Zinc transporter-1 concentrates at the postsynaptic density of hippocampal synapses. *Mol. Brain* **7,** 16 CrossRef Medline
16. Jirakulaporn, T., and Muslin, A. J. (2004) Cation diffusion facilitator proteins modulate Raf-1 activity. *J. Biol. Chem.* **279,** 27807–27815 CrossRef Medline
17. Beharier, O., Dror, S., Levy, S., Kahn, J., Mor, M., Etzion, S., Gitler, D., Katz, A., Muslin, A. J., Moran, A., and Etzion, Y. (2012) ZnT-1 protects HL-1 cells from simulated ischemia-reperfusion through activation of Ras-ERK signaling. *J. Mol Med. (Berl).* **90,** 127–138 Medline
18. Bruinsma, J. J., Jirakulaporn, T., Muslin, A. J., and Kornfeld, K. (2002) Zinc ions and cation diffusion facilitator proteins regulate Ras-mediated signaling. *Dev. Cell* **2,** 567–578 CrossRef Medline
19. Andrews, G. K., Wang, H., Dey, S. K., and Palmiter, R. D. (2004) Mouse zinc transporter 1 gene provides an essential function during early embryonic development. *Genesis* **40,** 74–81 CrossRef Medline
20. Hennigar, S. R., and McClung, J. P. (2016) Hepcidin attenuates zinc efflux in Caco-2 cells. *J. Nutr.* **146,** 2167–2173 CrossRef Medline
21. Levy, S., Beharier, O., Etzion, Y., Mor, M., Buzaglo, L., Shaltiel, L., Gheber, L. A., Kahn, J., Muslin, A. J., Katz, A., Gitler, D., and Moran, A. (2009) Molecular basis for zinc transporter 1 action as an endogenous inhibitor of L-type calcium channels. *J. Biol. Chem.* **284,** 32434–32443 CrossRef Medline
22. Lazarczyk, M., Pons, C., Mendoza, J. A., Cassonnet, P., Jacob, Y., and Favre, M. (2008) Regulation of cellular zinc balance as a potential mechanism of EVER-mediated protection against pathogenesis by cutaneous oncogenic human papillomaviruses. *J. Exp. Med.* **205,** 35–42 CrossRef Medline
23. Langmade, S. J., Ravindra, R., Daniels, P. J., and Andrews, G. K. (2000) The transcription factor MTF-1 mediates metal regulation of the mouse ZnT1 gene. *J. Biol. Chem.* **275,** 34803–34809 CrossRef Medline
24. Li, Y., Kimura, T., Huyck, R. W., Laity, J. H., and Andrews, G. K. (2008) Zinc-induced formation of a coactivator complex containing the zinc-

sensing transcription factor MTF-1, p300/CBP, and Sp1. *Mol. Cell Biol.* **28,** 4275–4284 CrossRef Medline

25. Hardyman, J. E., Tyson, J., Jackson, K. A., Aldridge, C., Cockell, S. J., Wakeling, L. A., Valentine, R. A., and Ford, D. (2016) Zinc sensing by metal-responsive transcription factor 1 (MTF1) controls metallothionein and ZnT1 expression to buffer the sensitivity of the transcriptome response to zinc. *Metallomics* **8,** 337–343 CrossRef Medline
26. Nishito, Y., Tsuji, N., Fujishiro, H., Takeda, T. A., Yamazaki, T., Teranishi, F., Okazaki, F., Matsunaga, A., Tuschl, K., Rao, R., Kono, S., Miyajima, H., Narita, H., Himeno, S., and Kambe, T. (2016) Direct comparison of manganese detoxification/efflux proteins and molecular characterization of ZnT10 as a manganese transporter. *J. Biol. Chem.* **291,** 14773–14787 CrossRef Medline
27. Fujimoto, S., Itsumura, N., Tsuji, T., Anan, Y., Tsuji, N., Ogra, Y., Kimura, T., Miyamae, Y., Masuda, S., Nagao, M., and Kambe, T. (2013) Cooperative functions of ZnT1, metallothionein and ZnT4 in the cytoplasm are required for full activation of TNAP in the early secretory pathway. *PLoS ONE* **8,** e77445 CrossRef Medline
28. Kambe, T., Suzuki, T., Nagao, M., and Yamaguchi-Iwai, Y. (2006) Sequence similarity and functional relationship among eukaryotic ZIP and CDF transporters. *Genomics Proteomics Bioinformatics* **4,** 1–9 CrossRef Medline
29. Fukue, K., Itsumura, N., Tsuji, N., Nishino, K., Nagao, M., Narita, H., and Kambe, T. (2018) Evaluation of the roles of the cytosolic N-terminus and His-rich loop of ZNT proteins using ZNT2 and ZNT3 chimeric mutants. *Sci. Rep.* **8,** 14084 CrossRef Medline
30. Liuzzi, J. P., Blanchard, R. K., and Cousins, R. J. (2001) Differential regulation of zinc transporter 1, 2, and 4 mRNA expression by dietary zinc in rats. *J. Nutr.* **131,** 46–52 CrossRef Medline
31. Laity, J. H., and Andrews, G. K. (2007) Understanding the mechanisms of zinc-sensing by metal-response element binding transcription factor-1 (MTF-1). *Arch. Biochem. Biophys.* **463,** 201–210 CrossRef Medline
32. Choi, S., and Bird, A. J. (2014) Zinc'ing sensibly: controlling zinc homeostasis at the transcriptional level. *Metallomics* **6,** 1198–1215 CrossRef Medline
33. Sankavaram, K., and Freake, H. C. (2012) The effects of transformation and ZnT-1 silencing on zinc homeostasis in cultured cells. *J. Nutr. Biochem.* **23,** 629–634 CrossRef Medline
34. Petris, M. J., Mercer, J. F., Culvenor, J. G., Lockhart, P., Gleeson, P. A., and Camakaris, J. (1996) Ligand-regulated transport of the Menkes copper P-type ATPase efflux pump from the Golgi apparatus to the plasma membrane: a novel mechanism of regulated trafficking. *EMBO J.* **15,** 6084–6095 CrossRef Medline
35. Yi, L., and Kaler, S. (2014) ATP7A trafficking and mechanisms underlying the distal motor neuropathy induced by mutations in ATP7A. *Ann. N.Y. Acad. Sci.* **1314,** 49–54 CrossRef Medline
36. Petris, M. J., Voskoboinik, I., Cater, M., Smith, K., Kim, B. E., Llanos, R. M., Strausak, D., Camakaris, J., and Mercer, J. F. (2002) Copper-regulated trafficking of the Menkes disease copper ATPase is associated with formation of a phosphorylated catalytic intermediate. *J. Biol. Chem.* **277,** 46736–46742 CrossRef Medline
37. Skjørringe, T., Amstrup Pedersen, P., Salling Thorborg, S., Nissen, P., Gourdon, P., and Birk Møller, L. (2017) Characterization of ATP7A missense mutants suggests a correlation between intracellular trafficking and severity of Menkes disease. *Sci. Rep.* **7,** 757 CrossRef Medline
38. Hogstrand, C., Kille, P., Nicholson, R. I., and Taylor, K. M. (2009) Zinc transporters and cancer: a potential role for ZIP7 as a hub for tyrosine kinase activation. *Trends Mol. Med.* **15,** 101–111 CrossRef Medline
39. Kambe, T., and Andrews, G. K. (2009) Novel proteolytic processing of the ectodomain of the zinc transporter ZIP4 (SLC39A4) during zinc deficiency is inhibited by acrodermatitis enteropathica mutations. *Mol. Cell Biol.* **29,** 129–139 CrossRef Medline
40. Hashimoto, A., Nakagawa, M., Tsujimura, N., Miyazaki, S., Kizu, K., Goto, T., Komatsu, Y., Matsunaga, A., Shirakawa, H., Narita, H., Kambe, T., and Komai, M. (2016) Properties of Zip4 accumulation during zinc deficiency and its usefulness to evaluate zinc status: a study of the effects of zinc deficiency during lactation. *Am. J. Physiol. Regul. Integr. Comp. Physiol.* **310,** R459–R468 CrossRef Medline
41. Lopez, V., and Kelleher, S. L. (2009) Zinc transporter-2 (ZnT2) variants are localized to distinct subcellular compartments and functionally transport zinc. *Biochem. J.* **422,** 43–52 CrossRef Medline
42. Zhao, N., Zhang, A. S., Worthen, C., Knutson, M. D., and Enns, C. A. (2014) An iron-regulated and glycosylation-dependent proteasomal degradation pathway for the plasma membrane metal transporter ZIP14. *Proc. Natl. Acad. Sci. U.S.A.* **111,** 9175–9180 CrossRef Medline
43. Hashimoto, A., Ohkura, K., Takahashi, M., Kizu, K., Narita, H., Enomoto, S., Miyamae, Y., Masuda, S., Nagao, M., Irie, K., Ohigashi, H., Andrews, G. K., and Kambe, T. (2015) Soybean extracts increase cell surface ZIP4 abundance and cellular zinc levels: a potential novel strategy to enhance zinc absorption by ZIP4 targeting. *Biochem. J.* **472,** 183–193 CrossRef Medline
44. Weaver, B. P., Dufner-Beattie, J., Kambe, T., and Andrews, G. K. (2007) Novel zinc-responsive post-transcriptional mechanisms reciprocally regulate expression of the mouse Slc39a4 and Slc39a5 zinc transporters (Zip4 and Zip5). *Biol. Chem.* **388,** 1301–1312 Medline
45. Dufner-Beattie, J., Wang, F., Kuo, Y. M., Gitschier, J., Eide, D., and Andrews, G. K. (2003) The acrodermatitis enteropathica gene ZIP4 encodes a tissue-specific, zinc-regulated zinc transporter in mice. *J. Biol. Chem.* **278,** 33474–33481 CrossRef Medline
46. Mao, X., Kim, B. E., Wang, F., Eide, D. J., and Petris, M. J. (2007) A histidine-rich cluster mediates the ubiquitination and degradation of the human zinc transporter, hZIP4, and protects against zinc cytotoxicity. *J. Biol. Chem.* **282,** 6992–7000 CrossRef Medline
47. Küry, S., Dréno, B., Bézieau, S., Giraudet, S., Kharfi, M., Kamoun, R., and Moisan, J. P. (2002) Identification of SLC39A4, a gene involved in acrodermatitis enteropathica. *Nat. Genet.* **31,** 239–240 CrossRef Medline
48. Wang, K., Zhou, B., Kuo, Y. M., Zemansky, J., and Gitschier, J. (2002) A novel member of a zinc transporter family is defective in acrodermatitis enteropathica. *Am. J. Hum. Genet.* **71,** 66–73 CrossRef Medline
49. Geiser, J., Venken, K. J., De Lisle, R. C., and Andrews, G. K. (2012) A mouse model of acrodermatitis enteropathica: loss of intestine zinc transporter ZIP4 (Slc39a4) disrupts the stem cell niche and intestine integrity. *PLoS Genet.* **8,** e1002766 CrossRef Medline
50. Nishito, Y., and Kambe, T. (2018) Absorption mechanisms of iron, copper, and zinc: an overview. *J. Nutr. Sci. Vitaminol. (Tokyo)* **64,** 1–7 Medline
51. Maryon, E. B., Molloy, S. A., and Kaplan, J. H. (2007) *O*-Linked glycosylation at threonine 27 protects the copper transporter hCTR1 from proteolytic cleavage in mammalian cells. *J. Biol. Chem.* **282,** 20376–20387 CrossRef Medline
52. Takeda, T. A., Miyazaki, S., Kobayashi, M., Nishino, K., Goto, T., Matsunaga, M., Ooi, M., Shirakawa, H., Tani, F., Kawamura, T., Komai, M., and Kambe, T. (2018) Zinc deficiency causes delayed ATP clearance and adenosine generation in rats and cell culture models. *Commun. Biol.* **1,** 113 CrossRef Medline
53. Yamazaki, T., Souquere, S., Chujo, T., Kobelke, S., Chong, Y. S., Fox, A. H., Bond, C. S., Nakagawa, S., Pierron, G., and Hirose, T. (2018) Functional domains of NEAT1 architectural lncRNA induce paraspeckle assembly through phase separation. *Mol. Cell* **70,** 1038–1053.e7 CrossRef Medline
54. Fukunaka, A., Kurokawa, Y., Teranishi, F., Sekler, I., Oda, K., Ackland, M. L., Faundez, V., Hiromura, M., Masuda, S., Nagao, M., Enomoto, S., and Kambe, T. (2011) Tissue nonspecific alkaline phosphatase is activated via a two-step mechanism by zinc transport complexes in the early secretory pathway. *J. Biol. Chem.* **286,** 16363–16373 CrossRef Medline
55. Devergnas, S., Chimienti, F., Naud, N., Pennequin, A., Coquerel, Y., Chantegrel, J., Favier, A., and Seve, M. (2004) Differential regulation of zinc efflux transporters ZnT-1, ZnT-5 and ZnT-7 gene expression by zinc levels: a real-time RT-PCR study. *Biochem. Pharmacol.* **68,** 699–709 CrossRef Medline
56. Fujimoto, S., Tsuji, T., Fujiwara, T., Takeda, T. A., Merriman, C., Fukunaka, A., Nishito, Y., Fu, D., Hoch, E., Sekler, I., Fukue, K., Miyamae, Y., Masuda, S., Nagao, M., and Kambe, T. (2016) The PP-motif in luminal loop 2 of ZnT transporters plays a pivotal role in TNAP activation. *Biochem. J.* **473,** 2611–2621 CrossRef Medline

Zinc transporter 1 (ZNT1) expression on the cell surface is elaborately controlled by cellular zinc levels

Yukina Nishito and Taiho Kambe

J. Biol. Chem. 2019, 294:15686-15697.
doi: 10.1074/jbc.RA119.010227 originally published online August 30, 2019